JACS
JOURNAL OF THE AMERICAN CHEMICAL SOCIETY
Article
pubs.acs.org/JACS

A Switchable Molecular Rotator: Neutron Spectroscopy Study on a Polymeric Spin-Crossover Compound

J. Alberto Rodríguez-Velamazán,*[,#] Miguel A. González,[‖] José A. Real,*[,†] Miguel Castro,[#] M. Carmen Muñoz,[‡] Ana B. Gaspar,[†] Ryo Ohtani,[⊥] Masaaki Ohba,*[,⊗] Ko Yoneda,[⊗] Yuh Hijikata,[⊥] Nobuhiro Yanai,[⊥] Motohiro Mizuno,[§] Hideo Ando,[▽] and Susumu Kitagawa[⊥]

[#]Instituto de Ciencia de Materiales de Aragón (ICMA), CSIC−Universidad de Zaragoza, 50009 Zaragoza, Spain

[‖]Institut Laue-Langevin, 38042 Grenoble Cedex 9, France

[†]Instituto de Ciencia Molecular (ICMol), Universidad de Valencia, E-46980 Paterna, Valencia, Spain

[‡]Departamento de Física Aplicada, Universidad Politécnica de Valencia, E-46022, Valencia, Spain

[⊥]Department of Synthetic Chemistry and Biological Chemistry and [▽]Department of Molecular Engineering, Graduate School of Engineering, Kyoto University, Katsura, Nishikyo-ku, Kyoto 615-8510, Japan

[⊗]Department of Chemistry, Faculty of Science, Kyushu University, Hakozaki, Higashi-ku, Fukuoka 812-8581, Japan

[§]Department of Chemistry, Graduate School of Natural Science & Technology, Kanazawa University, Kakuma, Kanazawa, Ishikawa 920-1192, Japan

Supporting Information

ABSTRACT: A quasielastic neutron scattering and solid-state ^{2}H NMR spectroscopy study of the polymeric spin-crossover compound {Fe(pyrazine)-[Pt(CN)$_4$]} shows that the switching of the rotation of a molecular fragment—the pyrazine ligand—occurs in association with the change of spin state. The rotation switching was examined on a wide time scale (10^{-13}–10^{-3} s) by both techniques, which clearly demonstrated the combination between molecular rotation and spin-crossover transition under external stimuli (temperature and chemical). The pyrazine rings are seen to perform a 4-fold jump motion about the coordinating nitrogen axis in the high-spin state. In the low-spin state, however, the motion is suppressed, while when the system incorporates benzene guest molecules, the movements of the system are even more restricted.

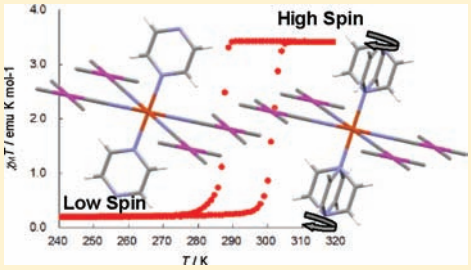

INTRODUCTION

One of the most important features of molecular materials is the possibility of combining different properties in a synergic way, giving a multifunctional material. Spin-crossover (SCO) compounds are particularly interesting to obtain these combinations of properties since their molecular bistability can be used to switch a second physical property by applying an external perturbation (temperature, pressure, or light irradiation). The SCO phenomenon is well known in Fe^{2+} coordination compounds, whose electronic configurations can move between high-spin (HS) and low-spin (LS) states under external stimuli, affording changes in magnetic, optical, dielectric, and structural properties.[1] When the cooperativity of the SCO is large enough, these compounds present a first-order spin transition (ST) with hysteretic behavior, conferring bistability and a memory function to the material.

Based on the classical Hofmann clathrate compounds,[2] the rigid 3D SCO frameworks {Fe(pz)[M^{II}(CN)$_4$]} (pz = pyrazine; M^{II} = Ni, Pd, Pt)[3] constitute one of the most interesting families in the quest for the aforementioned objective of multifunctionality. These coordination polymers display cooperative magnetic and chromatic thermal- and light-induced ST in the room-temperature region.[3,4] {Fe(pz)[Pt-(CN)$_4$]} (**1**) is particularly attractive, as it combines its SCO properties with guest adsorption processes, displaying a bidirectional chemoswitching between its HS and LS states.[5] This compound can also chemi-adsorb halogen molecules on its open metal sites of Pt, opening a way for sequestering and sensing of halogens.[6] In addition, it can be nanostructured as a thin film[4b,c] or nanocrystals[7] while preserving its SCO properties, enabling the material to be conveniently integrated into a functional device. Here we report another exciting property of this system: the possibility of switching the rotational motion of a molecular fragment—the pz rings—when switching the spin state by one of the mentioned external stimuli. Therefore, coming from the field of SCO compounds, this system converges with others of the most exciting branches of crystal engineering today: the construction of crystalline molecular rotators[8−13] in the quest for artificial crystalline molecular machines.[8]

Received: July 7, 2011
Published: February 24, 2012

   dx.doi.org/10.1021/ja206228n | J. Am. Chem. Soc. 2012, 134, 5083−5089

{Fe(pz)[Pt(CN)$_4$]} displays a first-order ST with a hysteresis of ~25 K wide (transition temperatures: $T_c^{\downarrow}$ = 285 ± 0.1 K and $T_c^{\uparrow}$ = 309 ± 0.1 K on cooling and warming, respectively). The crystallographic structure of **1**[5] can be described as 2D {Fe[Pt(CN)$_4$]}$_\infty$ layers connected along the (001) direction by the pyrazine ligands, which occupy the apical positions of the Fe octahedrons (Figure 1). The pz rings are rotationally

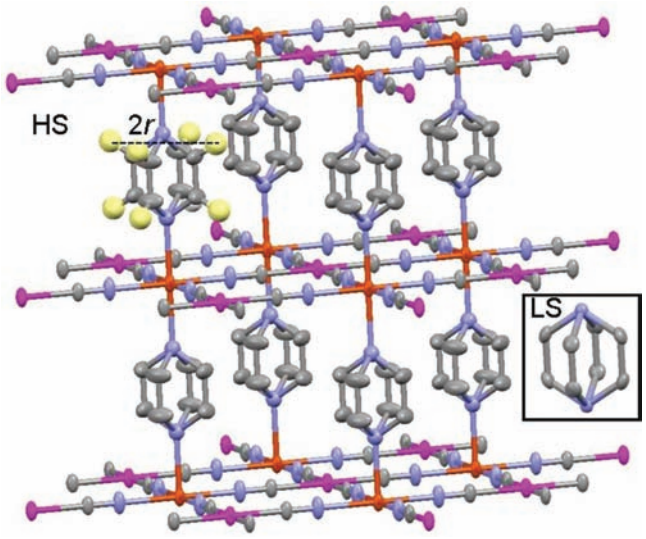

Figure 1. Crystal structure of **1**[5] in the HS state. Fe (orange), Pt (pink), N (blue), C (gray), H (yellow). The H atoms are omitted for clarity, except in one pz ring. Inset: detail of the thermal ellipsoids of the pz carbon atoms in the LS state.

disordered in both spin states, and this is reflected in the appearance of electronic density corresponding to the carbon atoms of the pz in two positions of the ring at 90° relative to each other. A similar situation was observed in the M^{II} = Ni related compound, where the presence of merohedral twinning resulted in an apparent tetragonal lattice and in excellent structural refinements with 50:50 occupation of orthogonal pz orientations.[14] Comparison of the thermal ellipsoids of the pz carbon atoms in the LS and HS states strongly suggests that this ligand rotates almost freely in the HS state, while rotation virtually disappears in the LS state (Figures 1 and S1). The connection of the mobility with the switch of the spin state is expected, taking into account that SCO is an entropy-driven phenomenon: The LS state is the ground state of the system at very low temperatures, while the HS state becomes the ground state at high temperatures. The difference in energy is thermally compensated by the higher entropy of the HS state, which mainly stems from electronic and vibrational contributions. In the case under study, the change in rotation velocity of the pz bridges may contribute considerably to this entropy variation, thereby influencing the ST process.

On the other hand, as a consequence of steric constraints in the pores, the adsorption of benzene (bz) in **1** produces the blocking of the system in HS state.[5] The guest bz molecules are believed to interpose between the pz rings, as occurs with the **1**·pz clathrate,[5] thus preventing the pz rings from rotating and hindering the shortening of the Fe−N bond distances. Despite the loss of entropy in this case due to restricted mobility of the pz rings, the HS state is favorable even at low temperatures because of the steric repulsion with the framework.[15]

Therefore, this system presents the phase order given by its rigid framework ("stator") and the molecular motility of an internal rotary element ("rotator"),[10] which are believed to be among the most important attributes for the design of artificial molecular machines.[9a,b] Moreover, in this compound the rigid framework can be significantly modified by inducing the ST, and hence the switching of the motion of the rotary elements becomes possible and occurs in combination with the changes in magnetic, optical, dielectric, and structural properties that characterize the SCO phenomenon. A different approach for combining molecular rotation and other physical properties (magnetic and electric) has also been reported using supramolecular rotators.[11]

In order to prove that there is a dynamic rotation and not only a static disorder, an unambiguous probe such as quasielastic neutron scattering (QENS) is needed. An analogous molecular rotator-like phenomenon was first described for the pyrazine rings of the system Mn[N(CN)$_2$]$_2$(pz)[12] by means of a QENS study. Also solid-state ^{2}H NMR spectroscopy is available for evaluating the ligand dynamics in porous frameworks.[13] In our work, we describe for the first time the coupling of this phenomenon with SCO; in other words, we demonstrate experimentally the bistability of rotation—immobility, which implies the possibility of switching the rotation at will. We therefore present a QENS (time scale 10^{-13}−10^{-8} s) and solid-state ^{2}H NMR (time scale 10^{-7}−10^{-3} s) study of the ligand dynamics of this system that evidences the rotation in the HS state of **1** and the loss of mobility in the LS state and in the bz clathrate, **1**·bz. The mobility change associated with ST was observed by both techniques, with QENS being used for the analysis of the HS state and ^{2}H NMR for the LS state, according to the different time scales.[16]

■ EXPERIMENTAL SECTION

Dehydrated microcrystalline {Fe(pz)[Pt(CN)$_4$]} (**1**) and its pyrazine-d_4 homologue {Fe(pz-d_4)[Pt(CN)$_4$]} (**1d**) were prepared as described elsewhere.[3,4d,5] The benzene clathrates {Fe(pz)[Pt(CN)$_4$](benzene)} (**1·bz**) and {Fe(pz-d_4)[Pt(CN)$_4$](benzene)} (**1d·bz**) were prepared by exposing **1** or **1d** to saturated benzene vapor for 1 h.[5]

The QENS experiments were performed in the direct time-of-flight spectrometer IN5 at the Institut Laue-Langevin (ILL, Grenoble, France). The wavelength of the incoming neutrons was 5 Å, resulting in an instrumental resolution (FWHM) of ~0.1 meV at the elastic line. The samples were placed inside identical annular aluminum sample holders and press-sealed with indium wire. The annular geometry was chosen to keep the scattering probability to ~0.1 in order to minimize multiple scattering effects. Temperature control was achieved using a standard ILL Orange cryostat. An empty aluminum can of the same dimension as the sample holder was measured and its spectrum subtracted from that of the sample. The detector efficiency was corrected using data collected from a standard vanadium sample, which is an elastic incoherent scatterer.

The data were reduced using LAMP[17] and the scattering function, $S(Q,\omega)$, spectra initially fitted to the sum of a delta-function and a Lorentzian peak both convoluted with the resolution function (estimated by the measurement of a vanadium sample), using the QENS_fit tool. Since we are only interested in incoherent scattering for the elastic incoherent structure factor (EISF), all spectra that have contributions from coherent scattering such as Bragg peaks were excluded from the fits. Once verified that the width of the Lorentzian peak, Γ_L, remains nearly constant, the number of adjustable parameters was reduced by constraining the fits to adjust Γ_L to the same value in the whole Q range. An example of the parameters obtained from this fit can be seen in the Supporting Information (Table S1). In a second step, the quasielastic part of the measured $S(Q,\omega)$ was analyzed using an expression specific for a 4-fold jump model.[18]

dx.doi.org/10.1021/ja206228n | J. Am. Chem. Soc. 2012, 134, 5083−5089

Solid-state ^{2}H NMR spectra of anhydrous **1d** and **1d·bz** were recorded in the 240−320 K temperature range on a Varian Chemagnetics CMX-300 spectrometer operated at 45.826 MHz, by quadrupole pulse sequence. The anhydrous samples were transferred to standard NMR tubes under N_2 gas. Simulated spectra were produced with FORTRAN original programs.[19]

RESULTS AND DISCUSSION

Quasielastic Neutron Scattering. The QENS technique consists of the analysis of the broadening of the elastic line (associated with neutrons scattered without energy transfer) produced by interactions of the neutrons with particles diffusing or reorienting in the probed material. With its characteristic energy scale and its high sensitivity to incoherent scattering from hydrogen nuclei, it is the ideal technique to probe the pz motions.

The scattered intensity is obtained experimentally for a given range of energy transfer, $\hbar\omega$, and momentum transfer, Q, in a single measurement using the neutron time-of-flight (TOF) technique. Since the incoherent cross section of hydrogen is much larger than that of other atoms, the measured scattering cross section is dominated by the incoherent scattering. This fact largely simplifies the analysis of quasielastic scattering data, as one can concentrate exclusively on the dynamics of the individual H atoms of the pz rings. The incoherent dynamical scattering function, $S^{inc}(Q,\omega)$ $(\approx S(Q,\omega))$, for such an incoherent scatterer undergoing reorientational motion may be described as a sum of two contributions: a single delta-function at zero energy transfer, of integrated area A_0, accounting for the elastic intensity (elastic structure factor), and a combination of Lorentzian contributions accounting for the quasielastic broadening related to the atomic motion (quasielastic structure factor):

$$S^{inc}(Q,\omega) = [A_0(Q)\delta(\omega) + S_{qel}(Q,\omega)] \quad (1)$$

Both parts are convoluted with the resolution function, $R(\omega)$, appropriate for the instrument, at each momentum transfer.[12,18]

The motion in the HS state and its practical disappearance in the LS state can be directly observed in the measurement of $S(Q,\omega)$ in the bistability region. As shown in Figure 2, (where the sum over Q, $S(\omega)$, of the quasielastic spectra is represented), while the width in LS practically corresponds to that of the resolution function (given by the measurement of a vanadium sample), a clear broadening is observed in HS state, proving unambiguously that part of the system is moving. For **1·bz**, the quasielastic broadening is still less than for **1** in the LS state, indicating the practical absence of mobility of the aromatic rings in this system.

The ratio of the elastic scattering to the total scattered intensity is the EISF, which using the appropriate normalization is equal to $A_0(Q)$. The Q-dependence of the EISF gives information about the geometry of the hydrogen motion.[18] For obtaining the EISF, the elastic and quasielastic parts can be estimated from the fitting of the measured $S(Q,\omega)$ to the sum of a delta-function and, as a first approximation, a single Lorentzian peak, L, of integrated area A_L and width Γ_L (both convoluted with the resolution function). The EISF of **1** is shown in Figure 3.

The presence of paramagnetic Fe^{2+} ions can give a quasielastic signal that complicates the analysis of the QENS spectra of **1** in terms of hydrogen motion. In this case, however, we can correct our data from this contribution by using the quasielastic intensity of **1·bz**, properly weighted in order to

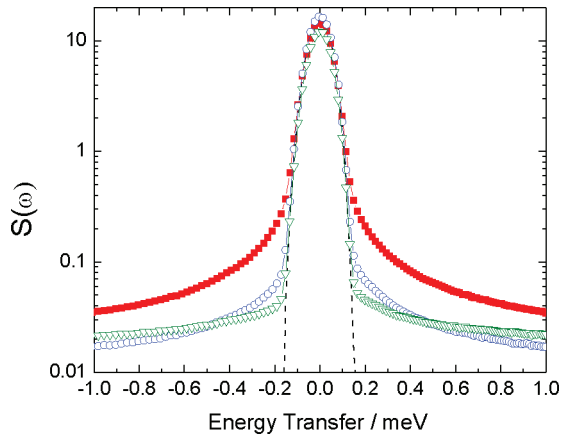

Figure 2. Quasielastic spectra at 295 K, summed over Q, of **1** in both the HS (squares) and LS (circles) states, and **1·bz** (triangles), together with the instrumental resolution given by the measurement of a vanadium foil (dashed line).

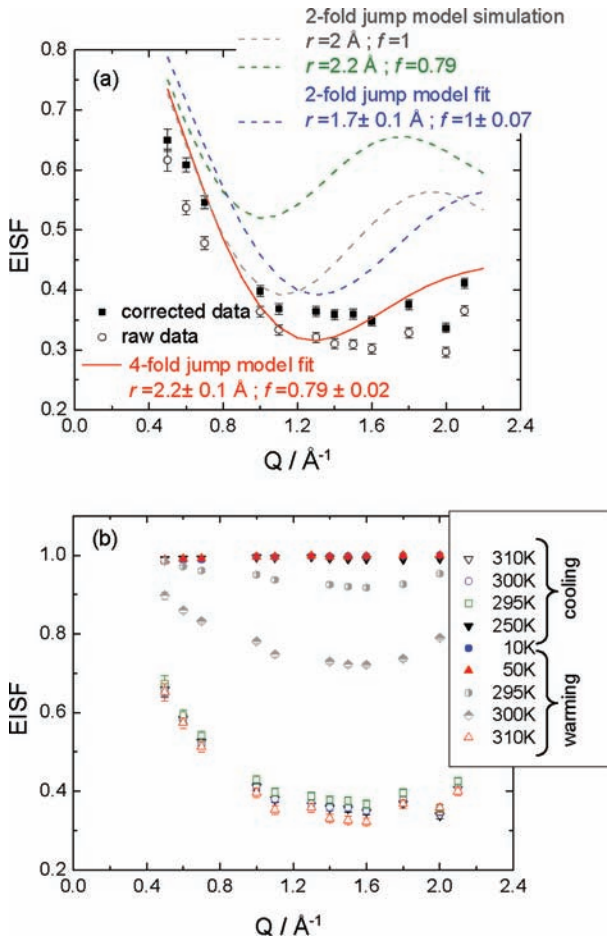

Figure 3. EISF of **1**. (a) EISF at 310 K in the HS state before and after correction from the paramagnetic contribution. The solid line is a fit to the 4-fold jump model described in eq 2, while the dashed lines are two simulations and a fit of the 2-fold jump model with different parameters. (b) EISF as a function of temperature. The open symbols correspond to the HS state and the full symbols to the LS state, and the half-full/half-open symbols stand for the system undergoing the spin transition.

dx.doi.org/10.1021/ja206228n | J. Am. Chem. Soc. 2012, 134, 5083−5089

account for the difference in hydrogen content in both compounds. As we have seen, the pz rings' motion is practically absent in **1·bz**, and therefore its quasielastic intensity should come from the paramagnetic Fe^{2+} ions and the aprotic ligands. Figure 3a shows the effect of this correction on the EISF of **1** at 310 K in the HS state.

Considering the crystallographic data, one can expect that the pz ligands perform rotations about the axis defined by the coordinating nitrogen atoms (C_4 axis). Actually, the width of the quasielastic peak is approximately constant over the entire Q-range, as is expected for this type of motion. Therefore, the H atoms will describe a circle of radius ∼2 Å, which corresponds to half of the H−H distance across the pz ring (Figure 1).[5] The obtained EISF (Figure 3a) could be fitted to a uniaxial rotational jump model between four sites equally spaced on a circle of radius r,[18] with an extra parameter f accounting for the fraction of the total number of H atoms that are moving:[12]

$$\begin{aligned}\mathrm{EISF} &= fA_0(Q) + (1-f)\\ &= f\frac{1}{4}[1 + 2j_0(Qr\sqrt{2}) + j_0(2Qr)] + (1-f)\end{aligned} \quad (2)$$

with $j_0(x)$ the spherical Bessel function ($j_0(x) = \sin(x)/x$). The necessity of this extra parameter f comes from the narrow energy resolution window of the instrument compared to the time scale of the hydrogen motion: at the studied temperatures, the time window of the instrument is short compared to the slow movement of the H atoms, and therefore only a part of these are seen moving. The best fit corresponds to $f = 0.79(2)$ and $r = 2.2(1)$ Å. Although the quality of the fit prevents us from using this method for calculating distances, the obtained r compares well with the value deduced from the neutron diffraction analysis of a similar compound, 2.08(1) Å.[20] The use of this distance as reference instead of that obtained for **1** in the X-ray diffraction (XRD) analysis[5] is justified by the fact that the distances obtained by neutron diffraction are longer than those obtained by XRD (up to ∼0.2 Å for the H−H distance across the pz ring[5,20]), as this last technique shows the electron density of an H atom at a mean position displaced toward the parent atom.[21]

The 4-fold jump model is physically grounded because, due to the symmetry of the system, the XRD experiments show the same electronic density in four equally spaced positions on the circle described by the H atoms, which suggest four equivalent energy minima in the circular path. This is consistent with the tendency of the pz ring to be either parallel or perpendicular, probably related with a steric effect between H atoms and CN groups. In principle, considering previous examples of similar compounds,[12] one could expect a motion of the H atoms based on the simplest model of 2-fold jumps. In Figure 3a, the results of the best fit to the 2-fold jump model are compared with those of the 4-fold jump model. The fit brings the f parameter to the upper limit ($f = 1$) and gives an unreasonable value for r (1.7(1) Å). For the shake of comparison, two simulations of the 2-fold jump model are also presented: with $f = 1$ and $r = 2$ Å, and with the same parameters obtained for the fit to the 4-fold jump model, $f = 0.79$ and $r = 2.2$ Å. As can be observed, the 2-fold jump model is discarded by our data, as the distinct minimum and the tendency toward one-half at high Q values characteristic of this model are not compatible with our results.

The temperature dependence of the EISF of **1** is shown in Figure 3b. In the LS state, the EISF remains constant and close to one, accordingly with a mainly elastic scattering coming from a practically immobile system. No changes are noticeable until 295 K on warming, where the EISF starts to show features of the HS state. In the HS state, the EISF remains very similar in the temperature range studied. Only a little tendency to decrease as the temperature increases can be perceived, which means that f increases with temperature; that is, as expected, the movements of the pz rings become faster at higher temperatures, and the fraction of H atoms whose movement can be observed in the time window of the instrument becomes higher.

Once the study of the EISF has allowed establishing the 4-fold jump model for the pz motion, a more accurate analysis of the quasielastic part of the measured $S(Q,\omega)$ can be performed in order to obtain quantitative information about the motion rate. The initial fitting using a single Lorentzian peak can be improved with the use of an expression specific for a 4-fold jump model for the quasielastic structure factor (the elastic part remains unaffected):[18]

$$S_{\mathrm{qel}}(Q,\omega) = [A_1(Q)L_1(\omega) + A_2(Q)L_2(\omega)] \quad (3.1)$$

with

$$A_1(Q) = \frac{1}{2}[1 - j_0(2Qr)] \quad (3.2)$$

$$A_2(Q) = \frac{1}{4}[1 - 2j_0(Qr2^{1/2}) + j_0(2Qr)] \quad (3.3)$$

while L_1 and L_2 are Lorentzian functions with half-width at half-maximum $1/\tau$ and $2/\tau$, respectively, τ being the average time spent by a proton in a site between two successive jumps. Constraining r to the value obtained by neutron diffraction (2.1 Å)[20] to avoid overparametrization of the fit, we obtain τ values ranging from 6.9(5) to 5.4(4) ps in the 295−320 K temperature range. Although the temperature range available is short, leading to a big error bar, an estimation of the activation energy (E_a) for rotation of pz in the HS state was obtained by an Arrhenius plot which gives $E_a = 1.7(5)$ kcal mol^{-1}, with a pre-exponential factor of 3×10^{12} Hz (Figure 4b). This value of E_a, which nicely agrees with that calculated theoretically by Ando et al. (cf. 1.1 kcal mol^{-1}),[15] is significantly lower than that observed—also by QENS—in the 180° jump motion of the pyrazine rings of the system $Mn[N(CN)_2]_2(pz)$ ($E_a = 5.7$ kcal mol^{-1}) and lies among the lowest reported in the literature for similar systems studied by NMR.[8,9,13]

^{2}H NMR Spectroscopy. The rotation of pz was also confirmed on the longer time scale by solid-state ^{2}H NMR spectroscopy, which is a powerful tool to examine the dynamics of frameworks in porous coordination polymers.[13] For this measurement we prepared $\{Fe(pz\text{-}d_4)[Pt(CN)_4]\}$ (**1d**) using deuterated pyrazine (pz-d_4) in the same way as **1**. This compound formed an isomorphously substituted structure of **1**, as checked by powder XRD. Also **1d** exhibited ST behavior similar to that of **1**, with $T_c^{\downarrow} = 288$ K and $T_c^{\uparrow} = 303$ K (Figure S2). ^{2}H NMR spectra of **1d** were measured in the temperature range of 240−320 K after evacuation by heating under reduced pressure. The line shape attributed to pz-d_4 changed from a distorted shape at 320 K to a symmetric shape with cooling to 240 K (Figures 4a and S4). The asymmetric line shape was recovered by heating to 300 K. The distorted line shape is attributable to a paramagnetic effect of the HS Fe(II) in the framework; on the other hand, the symmetric shape is attributable to a change of mobility of pz and vanishing of

dx.doi.org/10.1021/ja206228n | J. Am. Chem. Soc. 2012, 134, 5083−5089

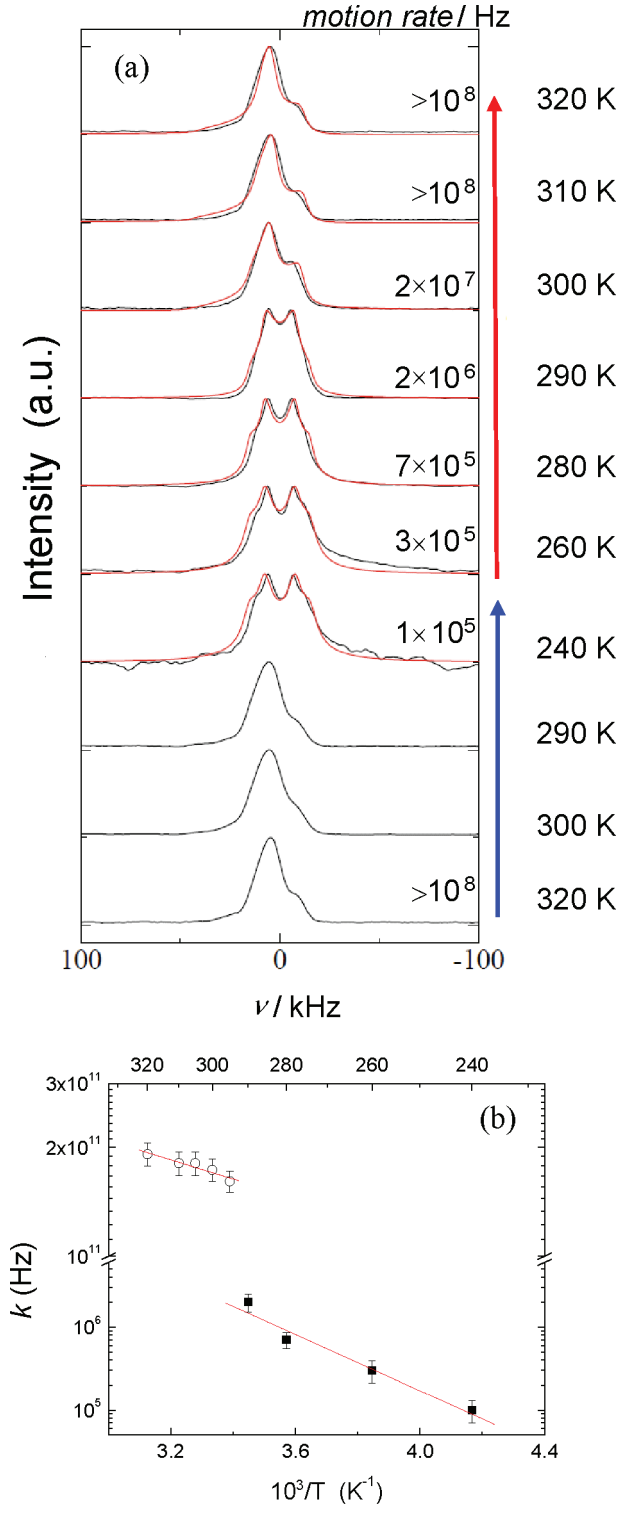

Figure 4. . (a) Experimental (black) and simulated (red) ^{2}H NMR spectra of **1d**. The red and blue arrows denote heating and cooling processes, respectively. (b) Arrhenius plot of the jumping rate k for 4-fold jumps in HS (circles, from QENS) and in LS (squares, from ^{2}H NMR).

the paramagnetic effect. More in detail, the line shape of the ^{2}H NMR spectrum in the diamagnetic LS state is dominated by only the quadrupole interaction and becomes symmetric. In the paramagnetic HS state, however, not only the quadrupole interaction but also the paramagnetic interaction (dipolar interaction between ^{2}H and paramagnetic Fe(II)) affects the line shape of the ^{2}H NMR spectrum. The dipolar interaction between ^{2}H and paramagnetic ion causes the asymmetric ^{2}H NMR line shape, since this interaction is anisotropic and the directions of its principal axes are different from those of the quadrupole interaction (Figure S7). The changes of spectra clearly trace the hysteretic ST behavior, with both line shapes observable in the region of 290 K, depending on the spin state of the system.

The spectra for the paramagnetic HS state were simulated as a four-site flip of pz rings along the C_4 axis, considering the contribution of paramagnetic shift of three kinds of nearest-neighbor iron atoms (Figure S7). The simpler 2-fold jump model was also simulated with flip angles of both 90° and 180°, but these simulations failed to reproduce the measured spectra (Figure S5). The distance and angle between deuterium and iron atoms for the simulation were taken from the crystal structure of **1**. The rotational rate, k, of pz was determined to be >10^8 Hz at 300 and 290 K in the hysteresis loop, beyond the limit of time scale of the technique. In the cooling process from 300 K, the rotation of pz was remarkably suppressed by the ST below 280 K. The symmetric spectra for the diamagnetic LS state were also analyzed as four-site flip motion and gave a rotational rate of 3 × 10^5 Hz at 260 K. In the heating process from 260 to 300 K, the rotational rate gradually increased with heating (7 × 10^5 Hz at 280 K and 2 × 10^6 Hz at 290 K), and then the shape returned to the initial distorted line shape at 300 K. The activation energy for rotation of pz in the LS state (heating process) was estimated to be 7.8(8) kcal mol^{-1} by an Arrhenius plot in the range of 240−290 K (Figure 4b), with a pre-exponential factor of 1.1 × 10^{12} Hz. The pre-exponential factors, very similar in the HS and LS states, agree well with the frequency derived from the moment of inertia of a pyrazine free rotator (2.5 × 10^{12} Hz).[22] On the other hand, the difference of the activation energy values in LS with those in HS is attributable to the contraction of the framework which occurs concomitantly with the SCO phenomenon. The shortening of the Fe−N(pz) distance (2.215(15) Å for the HS state and 1.985(16) Å for the LS state, see Figure S1) leads to an increase of the steric repulsion between pz and cyano groups in the LS state, which is the origin of the difference in activation barriers. The activation energy in **1d** is smaller than that observed by solid-state ^{2}H NMR in other systems with rotating pz, like $[Rh_2(O_2C\text{-}C_6H_5)_4(pz\text{-}d_4)]_n$ (E_a = 12 kcal mol^{-1}),[23] or with similarly large rotating organic fragments like the phenylene rings in mesoporous *p*-phenylenesilica (E_a = 13.2 kcal mol^{-1})[9e] or in 1,4-bis(triphenylsilylethynyl)benzene (E_a = 8.5 kcal mol^{-1}).[9f] In all these cases, the motion of the rings consists of 180° jumps, while 4-site jumps about a C_4 axis are observed in **1d**. Although the metal-binding sites of the cited rotational ligands are different, a reduction of the energy barrier like that observed could be expected as the rotational symmetry order is increased.[9f] The same effect can be invoked for explaining the difference of E_a between our **1** in HS and the system $Mn[N(CN)_2]_2(pz)$, both studied by QENS. An example of rotating pz with 4-site jump motion is that of $\{[CdNa(2\text{-}stp)(pz\text{-}d_4)_{0.5}(H_2O)](H_2O)\}_n$, with unusually small activation energy (E_a = 1.8 kcal mol^{-1}) and pre-exponential factor (2.4 × 10^6 Hz).[13a] In this case, however, this 4-site jump motion is asymmetric, and the inequality of the potential barriers between the four sites (asymmetric potential) might have an influence on these small values.

dx.doi.org/10.1021/ja206228n | J. Am. Chem. Soc. 2012, 134, 5083−5089

The dynamics of the benzene clathrate **1d·bz** was also measured at 290 K (Figure S6). In the same way as **1·bz**, **1d·bz** included one benzene and kept the HS state over the whole temperature range (Figure S2).[5] In the solid-state ^{2}H NMR measurement, the spectrum was asymmetric and dramatically broadened by the inclusion of bz, indicating that the rotation of pz was largely suppressed. The quantitative determination of the rotational mode of pz was difficult because of the partial release of bz under the measurement conditions. Further investigations, including measurements under equilibrium conditions in a sealed vial, are needed for clarifying the details of the influence of the guest on the dynamics of pz.

These ^{2}H NMR results clearly demonstrate the change of ligand dynamics in these porous frameworks under different spin states and are consistent with those of neutron spectroscopy, corroborating the switching of the rotation of pz associated with the ST. In this sense, although the results shown here support the 4-fold rotation model, the possibility of other types of rotation (for example, 2-fold jumps model with static disorder) does not change the main conclusion of this work, which is the activation/deactivation of the rotation upon ST.

An estimation of the entropic contribution related to the switching of the motion of pz, which is in the origin of the coupling between ST and pz rotation, can be obtained from the measured energy barriers in HS and LS by applying the method proposed by Ando et al.[15] This calculation (see Supporting Information) yields a rotational entropy of 1.90 cal mol^{-1} K^{-1} at room temperature, in good agreement with the value obtained theoretically (1.84 cal mol^{-1} K^{-1}).[15] The obtained rotational entropy value is as large as 9.4% of the total experimental entropy change in the ST of 20.32 cal mol^{-1} K^{-1} determined for single crystals of this compound,[4d] pointing out the crucial effect on the ST of the change in mobility of the pz rings.

CONCLUSIONS

In summary, we have shown by quasielastic neutron scattering and ^{2}H NMR spectroscopy that the switching of the rotation of a molecular fragment—the pz ligand—occurs in {Fe(pz)[Pt(CN)$_4$]} associated with the change of spin state. The rotation switching was examined on a wide time scale, 10^{-13}–10^{-8} s by QENS and 10^{-7}–10^{-3} s by solid-state ^{2}H NMR, which clearly demonstrated the combination between molecular rotation and spin transition under external stimuli (temperature and chemical). The pz rings are seen to perform a 4-fold jump motion about the coordinating nitrogen axis in the high-spin state. In the low-spin state, however, the motion is suppressed, and when the system incorporates benzene guest molecules, the movements of the system are even more restricted. The correlation between rotation of pz and the change of spin state in SCO systems can be a practical element for creating artificial molecular machines.

ASSOCIATED CONTENT

Supporting Information

Additional crystallographic information, magnetic susceptibility data of the deuterated sample, details of the fits of QENS data, ^{2}H-NMR spectrum of **1d·bz**, detailed description of the simulation procedure for the ^{2}H-NMR spectra and details of the calculation of the rotational entropy. This material is available free of charge via the Internet at http://pubs.acs.org.

AUTHOR INFORMATION

Corresponding Author

jarv@unizar.es

Notes

The authors declare no competing financial interest.

ACKNOWLEDGMENTS

This work was supported by the Spanish MICINN and FEDER, projects MAT2007-61621, CSD2007-00010, MAT2011-27233-C02-02, and CTQ2010-18414, and by a CREST JST program and Grant-In-Aid for Scientific Research (No. 23245014 and 22108512) from the Ministry of Education, Culture, Sports, Science and Technology of Japan. The Institut Laue-Langevin is acknowledged for neutron beam time allocation.

REFERENCES

(1) *Spin-Crossover in Transition Metal Compounds*; Vols. *I*–*III*, Topics in Current Chemistry; Gütlich, P., Goodwin, H. A., Eds.; Springer: Berlin, 2004.

(2) Hofmann, K. A.; Küspert, F. *Z. Anorg. Allg. Chem.* **1897**, *15*, 204.

(3) Niel, V.; Martínez-Agudo, J. M.; Muñoz, M. C.; Gaspar, A. B.; Real, J. A. *Inorg. Chem.* **2001**, *40*, 3838–3839.

(4) (a) Cobo, S.; Ostrovskii, D.; Bonhommeau, S.; Vendier, L.; Molnár, G.; Salmon, L.; Tanaka, K.; Bousseksou, A. *J. Am. Chem. Soc.* **2008**, *130*, 9019–9024. (b) Molnár, G.; Cobo, S.; Real, J. A.; Carcenac, F.; Daran, E.; Vieu, C.; Bousseksou, A. *Adv. Mater.* **2007**, *19*, 2163. (c) Bonhommeau, S.; Molnár, G.; Galet, A.; Zwick, A.; Real, J. A.; McGarvey, J. J.; Bousseksou, A. *Angew. Chem., Int. Ed.* **2005**, *44*, 2. (d) Tayagaki, T.; Galet, A.; Molnár, G.; Muñoz, M. C.; Zwick, A.; Tanaka, K.; Real, J. A.; Bousseksou, A. *J. Phys. Chem. B* **2005**, *109*, 14859.

(5) Ohba, M.; Yoneda, K.; Agustí, G.; Muñoz, M. C.; Gaspar, A. B.; Real, J. A.; Yamasaki, M.; Ando, H.; Nakao, Y.; Sakaki, S.; Kitagawa, S. *Angew. Chem., Int. Ed.* **2009**, *48*, 4767–4771.

(6) (a) Agustí, G.; Ohtani, R.; Yoneda, K.; Gaspar, A. B.; Ohba, M.; Sánchez-Royo, J. F.; Muñoz, M. C.; Kitagawa, S.; Real, J. A. *Angew. Chem., Int. Ed.* **2009**, *48*, 8944–8947. (b) Ohtani, R.; Yoneda, K.; Furukawa, S.; Horike, N.; Kitagawa, S.; Gaspar, A. B.; Muñoz, M. C.; Real, J. A.; Ohba, M. *J. Am. Chem. Soc.* **2011**, *133*, 8600–8605.

(7) (a) Boldog, I.; Gaspar, A. B.; Martínez, V.; Pardo-Ibáñez, P.; Ksenofontov, V.; Bhattacharjee, A.; Gütlich, P.; Real, J. A. *Angew. Chem., Int. Ed.* **2008**, *47*, 6433–6437. (b) Volatron, F.; Catala, L.; Rivière, E.; Gloter, A.; Stephan, O.; Mallah, T. *Inorg. Chem.* **2008**, *47*, 6584–6586.

(8) *Molecular Machines*; Vol. *262*, Topics in Current Chemistry; Kelly, T. R., Ed.; Springer: Berlin, 2005.

(9) (a) Garcia-Garibay, M. A. *Proc. Natl. Acad. Sci. U.S.A.* **2005**, *102*, 10771. (b) Garcia-Garibay, M. A. *Angew Chem., Int. Ed.* **2007**, *46*, 8945. (c) Garcia-Garibay, M. A. *Nat. Mater.* **2008**, *7*, 431. (d) Gould, S. L.; Tranchemontagne, D.; Yaghi, O. M.; Garcia-Garibay, M. A. *J. Am. Chem. Soc.* **2008**, *130*, 3246–3247. (e) Comotti, A.; Bracco, S.; Valsesia, P.; Beretta, M.; Sozzani, P. *Angew. Chem., Int. Ed.* **2010**, *49*, 1760. (f) Karlen, S. D.; Reyes, H.; Taylor, R. E.; Khan, S. I.; Hawthorne, M. F.; Garcia-Garibay, M. A. *Proc. Natl. Acad. Sci. U.S.A.* **2010**, *107*, 14973–14977.

(10) Kottas, G. S.; Clarke, L. I.; Horinek, D.; Michl, J. *Chem. Rev.* **2005**, *105*, 1281.

(11) (a) Endo, T.; Akutagawa, T.; Noro, S.; Nakamura, T. *Dalton Trans.* **2011**, *40*, 1491–1496. (b) Akutagawa, T.; Sato, D.; Ye, Q.; Endo, T.; Noro, S.; Takeda, S.; Nakamura, T. *Dalton Trans.* **2010**, *39*, 8219–8227. (c) Akutagawa, T.; Sato, D.; Koshinaka, H.; Aonuma, M.; Noro, S.; Takeda, S.; Nakamura, T. *Inorg. Chem.* **2008**, *47*, 5951–5962. (d) Nishihara, S.; Akutagawa, T.; Sato, D.; Takeda, S.; Noro, S.; Nakamura, T. *Chem. Asian J.* **2007**, *2*, 1083–1090. (e) Akutagawa, T.; Koshinaka, H.; Sato, D.; Takeda, S.; Noro, S. I.; Takahashi, H.; Kumai, R.; Tokura, Y.; Nakamura, T. *Nat. Mater.* **2009**, *8*, 342–347.

(f) Akutagawa, T.; Shitagami, K.; Nishihara, S.; Takeda, S.; Hasegawa, T.; Nakamura, T.; Hosokoshi, Y.; Inoue, K.; Ikeuchi, S.; Miyazaki, Y; Saito, K. *J. Am. Chem. Soc.* **2005**, *127*, 4397−4402.
(12) Brown, C.; Manson, J. L. *J. Am. Chem. Soc.* **2002**, *124*, 12600−12605.
(13) (a) Horike, S.; Matsuda, R.; Tanaka, D.; Matsubara, S.; Mizuno, M.; Endo, K.; Kitagawa, S. *Angew. Chem., Int. Ed.* **2006**, *45*, 7226−7230. (b) Horike, S.; Shimomura, S.; Kitagawa, S. *Nature Chem.* **2009**, *1*, 695−704. (c) Kolokolov, D. I.; Jobic, H.; Stepanov, A. G.; Guillerm, V.; Devic, T.; Serre, C.; Férey, G. *Angew. Chem., Int. Ed.* **2010**, *49*, 4791−4794.
(14) Southon, P. D.; Liu, L.; Fellows, E. A.; Price, D. J.; Halder, G. J.; Chapman, K. W.; Moubaraki, B.; Murray, K. S.; Létard, J.-F.; Kepert, C. J. *J. Am. Chem. Soc.* **2009**, *131*, 10998.
(15) Ando, H.; Nakao, Y.; Sato, H.; Ohba, M.; Kitagawa, S.; Sakaki, S. *Chem. Phys. Lett.* **2011**, *511*, 399−404.
(16) *Nuclear Magnetic Resonance Probes of Molecular Dynamics*; Tycko, R., Ed.; Springer: Berlin, 1994.
(17) LAMP, the Large Array Manipulation Program (http://www.ill.fr/data_treat/lamp/lamp.html).
(18) Bée, M. *Quasielastic Neutron Scattering*; Adam Hilger: Bristol, 1988.
(19) Mizuno, M.; Itakura, N.; Endo, K. *Chem. Phys. Lett.* **2005**, *416*, 358−363.
(20) Manson, J. L.; Huang, Q.-z.; Lynn, J. W.; Koo, H.-J.; Whangbo, M.-H.; Bateman, R.; Otsuka, T.; Wada, N.; Argyriou, D. N.; Miller, J. S. *J. Am. Chem. Soc.* **2001**, *123*, 162.
(21) Cotton, F. A.; Falvello, L. R.; Murillo, C. A.; Pascual, I.; Schultz, A. J.; Tomás, M. *Inorg. Chem.* **1994**, *33*, 5391−5395.
(22) The frequency of free rotation, k_{FR}, of the pyrazine rings was calculated from the moment of inertia I along the N−N axis with the relation $k_{FR} = (2\pi/9)(I/k_BT)^{1/2}$: Kawaski, A. *Crit. Rev. Anal. Chem.* **1993**, *23*, 459.
(23) Takamizawa, S.; Nataka, E.; Akatsuka, T.; Miyake, R.; Kakizaki, Y.; Takeuchi, H.; Maruta, G.; Takeda, S. *J. Am. Chem. Soc.* **2010**, *132*, 3783−3729.